James F. Reynolds John D. Tenhunen (Eds.)

# Landscape Function and Disturbance in Arctic Tundra

With 109 Figures, 11 in color
and 47 Tables

To Harbin,
With best regards and
compliments —
Jim

Springer

# 18 Road-Related Disturbances in an Arctic Watershed: Analyses by a Spatially Explicit Model of Vegetation and Ecosystem Processes

P. W. LEADLEY, H. LI, B. OSTENDORF, and J. F. REYNOLDS

J.F. Reynolds and J.D. Tenhunen (Eds.)
Ecological Studies, Vol. 120


## 18.1 Introduction

Landscape models have proven very useful in assessing historical change in vegetation patterns, for predicting the impacts of human disturbance on ecosystems, and for developing strategies to manage natural resources (e.g., Shugart 1984; Turner 1987; Costanza et al. 1990; Turner and Dale 1991; Wu and Levin 1994). Landscape models may implicitly or explicitly consider the *spatial heterogeneity* of system properties such as plant biomass, soil nutrient concentration, and topography – defined by either qualitative indices (e.g., patchiness, diversity, contagion) and/or quantitative indices (e.g., autocorrelation, variance, trend) (Li and Reynolds 1995). Accounting for such spatial heterogeneity has been shown to be essential for modeling ecosystem response to disturbance (Turner 1989; Costanza et al. 1990; Turner and Dale 1991; DeAngelis and White 1994). Although the use of simplified, aggregate models to represent vegetation and ecosystem processes (particularly at the scale of a landscape) has inherent dangers (Bonan 1993), the questions posed by resource managers require the development of models that summarize our "state-of-the-art" ecological knowledge and realistically represent the dynamic function of ecosystems in time and space.

Most existing ecosystem models for the Arctic emphasize properties at the level of the plant or plant community and do not incorporate landscape level properties (see review in Reynolds and Leadley 1992). Reich et al. (1991) and McGuire et al. (1992) parameterized a spatially explicit model for arctic ecosystems, but it did not include transport processes and operates at a grid size (0.5° latitude × 0.5° longitude) that is too large to assess the impacts of common disturbances (Fig. 3.2 in Chap. 3, this Vol.). In this chapter we present T-MAP (Terrain Models for Arctic Processes), a set of spatially explicit models for examining the effects of road construction on tundra ecosystems. T-MAP predicts landscape patterns of water discharge, nitrogen (N) availability, vegetation types, plant biomass, and net primary productivity within the Imnavait Creek watershed in the foothills of the Brooks Range in Alaska. The development of T-MAP was motivated by the R4D goal of predicting the potential effects of energy-related development on ecosystems of the North Slope of Alaska (Chaps. 1 and 14, this Vol.).

We describe T-MAP and present comparisons of simulated ecosystem properties with a vegetation index derived from satellite measurements of

spectral reflectance. We used T-MAP to explore the ecosystem consequences of several scenarios for hypothetical road construction through the Imnavait Creek watershed including: (1) the obstruction of natural water drainage, and (2) the deposition of dust originating from high-speed vehicle traffic. We focused on road-related disturbances, because the Dalton Highway that serves the trans-Alaskan pipeline is one of the most prominent energy-related ecosystem disturbances in the foothills of the Brooks Range (Chap. 3, this Vol.). Gravel roads built to support energy exploration in the Arctic alter ecosystem properties mainly by (1) disrupting natural water drainage and (2) via dust deposition that accompanies the high-speed vehicle traffic (Chap. 15, this Vol.). The disruption of water drainage can cause impoundments and result in severe thermal erosion (i.e., thermokarst) particularly in areas with massive ground ice (Sect. 3.3.4.7, this Vol.). Dust damages or eliminates most of the acidophyllic plant species, e.g., *Sphagnum* mosses and lichens (Walker and Everett 1987; Meininger and Spatt 1988; Sect. 3.3.4.6, this Vol.). Our simulations with T-MAP, although preliminary, provide information that may be useful for considering options for road placement across watersheds, and suggest that this modeling approach has high potential for development as a management tool in arctic landscapes.

## 18.2 Environmental Gradients and Vegetation Distribution

### 18.2.1 Vegetation and Topography

Walker et al. (1989) grouped the vegetation of the Brooks Range Foothills into five main classes:

1. Dry types dominated by ericaceous dwarf shrubs and lichens;
2. Moist types dominated by mesic dwarf shrubs, sedges, and mosses;
3. Wet types dominated by sedges, dwarf shrubs, and mosses;
4. Aquatic types dominated by sedges, grasses, or forbs;
5. Barren or partially vegetated areas.

In developing T-MAP we focused on the first three types following the definitions used by Oberbauer et al. (Chap. 11, this Vol.) and Ostendorf et al. (Chap. 17, this Vol.), i.e., we refer to the dry types as *heath*, the moist types as *tussock tundra*, and the wet types as *riparian*. These vegetation types account for more than 95% of the vegetation in the Imnavait Creek and adjacent watersheds (Walker et al. 1989; Chap. 4, this Vol.).

The Imnavait Creek watershed is elongated in the N–S direction with the creek running northward within the basin. Both ridges of the watershed are dominated by dry heath vegetation. The southwest facing slope is dominated by moist tussock tundra and is characterized by the presence of well-developed water tracks. The northeast facing slope of the watershed is steeper with a

relatively narrow band of tussock tundra vegetation separating heath from riparian vegetation. The watershed basin – characterized by very low slopes – is dominated by wet riparian vegetation.

### 18.2.2 Role of Water and Light

Soil moisture is one of the most important determinants of the distribution, biomass, and productivity of poikilohydric plants in the Arctic (Fig. 14.9, this Vol.). Along a moisture gradient in the Imnavait Creek watershed, Tenhunen et al. (1992) reported a transition from a lichen-dominated system (lowest water availability) to one dominated by *Sphagnum* moss, and then to one where poikilohydric plants were eliminated (highest water availability). Lichens are restricted to relatively dry sites, because mosses outcompete the slower growing lichens as surface moisture increases. Mosses grow in abundance in most tundra ecosystems with the exception of the driest and wettest habitats. Moss biomass and productivity generally increase with increasing moisture (Hastings et al. 1989; Murray et al. 1989), although biomass tends to decrease in the wettest sites. Light is also an important determinant of moss productivity. Shading by vascular plants may reduce moss biomass (Hastings et al. 1989), but may increase the productivity: biomass ratio (Harley et al. 1989; Murray et al. 1989).

### 18.2.3 Role of Nutrients

Although numerous process studies in the Arctic have established a strong relationship between water and plant structure and function, water per se does not strongly affect vascular plant productivity in most low arctic ecosystems. Much evidence suggests that N availability is the primary constraint on vascular plant productivity (e.g., Shaver and Chapin 1980; Shaver et al. 1986). Simulations of N uptake and movement in tussock tundra soils (Leadley et al. 1995) and simulations of the growth of *Eriophorum vaginatum* (Leadley and Reynolds 1992) suggest that (1) N uptake by tussock-tundra plants is primarily limited by the N availability in the soils, and not by plant uptake characteristics or root biomass, and (2) nitrogen – not $CO_2$ concentration, temperature, or radiation – is the primary determinant of plant growth.

There appears to be a strong relationship between water and nutrient availability in arctic tundra ecosystems. In field studies, the observed changes in vascular plant productivity, due to increased moisture, have also been attributed to increased nutrient availability (Chapin et al. 1988; Kielland and Chapin 1992; Oberbauer and Dawson 1992; Chap. 10, this Vol.). Chapin et al. (1988) found that areas of moist tundra where water is channeled (water tracks) have higher vascular productivity and N availability than areas that do not. Increased N availability in water tracks has been attributed to movement of N in water, increased thaw depth, warmer soil temperatures, and increased

N diffusion in the soil (Chapin et al. 1988; Oberbauer and Dawson 1992). Without water movement wet soils are associated with relatively low N availability, due to anaerobic conditions that inhibit microbial mineralization. In this case, decreases in soil moisture improve soil aeration and tend to enhance N availability (Kielland and Chapin 1992; Nadelhoffer et al. 1992).

## 18.3 Description of Model

### 18.3.1 Overview

T-MAP is based on the following assumptions:

1. "Average" soil moisture during the growing season, computed as the variable *Soil Mois*, can be derived from local water discharge and slope.
2. The pattern of vegetation types in arctic landscapes can be predicted from local water discharge and slope.
3. The productivity and biomass of poikilohydric plants can be directly related to soil moisture.
4. N availability can be related to soil moisture.
5. The long-term productivity of vascular plants in tundra ecosystems can be reasonably estimated from the amount of N available and the efficiency of N use in production.

These assumptions are based on the experimental and modeling results discussed in Section 18.2 and in Chapters 5 and 14 (this Vol.).

T-MAP is composed of four models (T-HYDRO, T-VEG, T-NUT, and T-PLT) that describe spatially explicit relationships between elevation, slope, soil moisture, vegetation types, N availability, and plant biomass and production for each of ca. 5200 pixels in the Imnavait Creek watershed map (see Fig. 18.1). The only inputs to T-MAP are the digital elevation model (DEM, ca. 20m × 20 m pixel size) and annual precipitation. All variables and parameters are defined in Table 18.1.

#### 18.3.1.1 T-HYDRO

T-HYDRO computes total *Discharge* for each pixel in the watershed as:

$$Discharge = Runon + Ppt - Evapo, \quad (1)$$

where *Discharge* is total volume of water ($m^3$ $pixel^{-1}$ or $m^3$ $20\,m^{-2}$), *Runon* is total runon, *Ppt* is precipitation and *Evapo* is evapotranspiration. Details and assumptions of the water-routing algorithm used in T-HYDRO are given in Ostendorf and Reynolds (1993), and a brief overview is provided in Chap. 14 (this Vol.). We assume no net change in water storage in a pixel during the time interval for which the budget is calculated (i.e., between years). Conceptually, all pixels are linked by a network of nodes (located at the center of a pixel) that

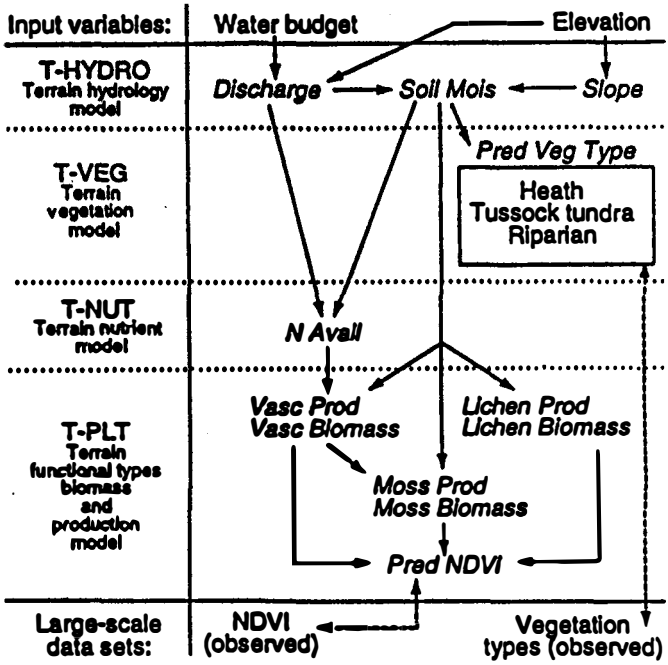


**Fig.18.1** Overview of models contained in terrain models for artic processes (T-MAP)

are connected by pipes of equal diameter filled with soil. The elevation difference between pixels is the gravitational potential between nodes. Darcy's law is used to estimate *Discharge* through these connections and, ultimately, its routing through the pixels of the landscape (Fig. 14.10 in Chap. 14, this Vol.). Model output is a two-dimensional "drainage area" map that gives total upslope discharge ($m^3$ water) from each pixel. In order to obtain units independent of pixel size, *Discharge* was scaled to units of $m^3\ m^{-1}$ (hereafter noted as *Discharge**) by multiplying by the length of a pixel (20 m; Quinn et al. 1991). The drainage map was scaled assuming $(Ppt - Evapo) = 0.098\ m^3 m^{-2}$ for each pixel based on the total 1986 discharge of 209 000 $m^3$ in Imnavait Creek (Chap. 6, this Vol.).

Following Burt and Butcher (1985) a simple index of average soil moisture, *Soil Mois*, is derived from Darcy's law as a function of *Discharge** and *Slope*. *Slope* determines the gravitational gradient that influences flow velocity. *Slope* was obtained from the Imnavait Creek DEM grid using the scheme described in Ostendorf and Reynolds (1995; see also Chap. 17, this Vol.). The index was modified because it appeared to overestimate soil moisture at low slopes and discharges in the Imnavait Creek catchment:

$$Soil\ Mois = \begin{cases} Discharge^* / S_{min} \text{ if } Discharge^* < D_{min} \text{ and } Slope < S_{min} \\ Dishcarge^* / Slope \text{ otherwise,} \end{cases} \quad (2)$$

Table 18.1. Variables and parameters in terrain models for arctic processes (T-MAP)

| Name | Description | Units/values |
|---|---|---|
| a | Intercept, Eq. (20) | 0.026 |
| b | Slope, Eq. (20) | $7 \times 10^{-4}$ m$^2$ year g$^{-1}$ |
| $D^{Biomass}_{Moss}$ | Effect of dust on moss biomass (Fig. 18.3) | 0–1 |
| $D^{Biomass}_{Lichen}$ | Effect of dust on lichen biomass (Fig. 18.3) | 0–1 |
| $D^{Frac}_{Sphag}$ | Effect of dust on the fraction of moss biomass that is *Sphagnum* (Fig. 18.3) | 0–1 |
| *Discharge* | Amount of water routed through a site | m$^3$ pixel$^{-1}$ year$^{-1}$ |
| *Discharge** | Amount of water routed through a site | m$^3$ m$^{-1}$ year$^{-1}$ |
| Dist | Distance from road | m |
| $D_{max}$ | Maximum dust load | 250 g m$^{-2}$ |
| $D_{min}$ | Parameter in *Soil Mois* calculations (Fig. 18.2) | 10 m$^3$ m$^{-1}$ |
| $D^{Prod}_{Vasc}$ | Effect of dust on vascular plant productivity | 0–1 |
| *Dust Load* | Dust deposition | g m$^{-2}$ |
| *Evapo* | Total evapotranspiration | m$^3$ pixel$^{-1}$ year$^{-1}$ |
| *Lichen Biom* | Live lichen biomass | g m$^{-2}$ |
| *Lichen Biom Max* | Maximum lichen biomass | 350 g m$^{-2}$ |
| *Lichen Prod* | Lichen productivity | g m$^{-2}$ year$^{-1}$ |
| $M^{Biomass}_{Lichen}$ | Effect of moisture on lichen biomass (Fig. 18.3) | 0–1 |
| $M^{Biomass}_{Moss}$ | Effect of moisture on moss biomass (Fig. 18.3) | 0–1 |
| $M^{Biomass}_{Vasc}$ | Effect of moisture on vascular plant biomass (Fig. 18.3) | 0–1 |
| $M^{Frac}_{Sphag}$ | Effect of moisture on the fraction of moss biomass that is *Sphagnum* (Fig. 18.3) | 0–1 |
| $M^{min}_N$ | Minimum value of $M_N$ (Fig. 18.3) | 0.55 |
| $M_N$ | Effect of *Soil Mois* on *N Avail* (Fig. 8.3) | 0–1 |
| *Moss Biom* | Live (i.e., green) moss biomass | g m$^{-2}$ |
| *Moss Biom Max* | Maximum moss biomass | 400 g m$^{-2}$ |
| *Moss Biom Sphag* | Biomass of the moss, *Sphagnum* | g m$^{-2}$ |
| *Moss Prod* | Moss productivity | g m$^{-2}$ year$^{-1}$ |
| *N Avail* | N availability | g m$^{-2}$ year$^{-1}$ |
| $N_{max}$ | Maximum nitrogen availability | 1.6 g m$^{-2}$ year$^{-1}$ |
| *NPP* | Net primary productivity | g m$^{-2}$ year$^{-1}$ |
| NUE | Nitrogen-use efficiency for vascular plants | 140 g dry weight g$^{-1}$ N |
| *Obs NDVI* | Observed normalized difference vegetation index derived from a SPOT/HRV-XS scheme June 22, 1987 (Stow et al. 1986) | – |
| *Obs Veg Type* | Observed vegetation type from Walker et al. (1989): heath, tussock tundra, or riparian | – |
| $PB_{Lichen}$ | Lichen productivity: biomass ratio | 0.025 year$^{-1}$ |
| $PB_{Moss}$ | Moss productivity: biomass ratio | 0.25 year$^{-1}$ |
| $PB_{Vasc}$ | Vascular plant productivity: biomass ratio | 0.25 year$^{-1}$ |
| *Ppt* | Total precipitation | m$^3$ pixel$^{-1}$ year$^{-1}$ |
| *Pred NDVI* | Predicted normalized difference vegetation index | – |
| *Pred Veg Type* | Predicted vegetation type: heath, tussock tundra, riparian | – |
| *Runon* | Total water run-on to a pixel | m$^3$ pixel$^{-1}$ year$^{-1}$ |
| $S^{Biomass}_{Moss}$ | Effect of shading on moss biomass (Fig. 18.3) | 0–1 |
| *Slope* | Slope | m m$^{-1}$ |
| $S_{min}$ | Parameter in *Soil Mois* calculations (Fig. 18.2) | 2 degrees |

Table 18.1. (*continued*)

| Name | Description | Units/values |
|---|---|---|
| *Soil Mois* | Soil moisture index | $m^3 m^{-1}$ degree$^{-1}$ |
| $S_{shad}$ | Effect of shading on moss productivity (Fig. 18.3) | 0–1 |
| *TAGB* | Total aboveground plant biomass | $g m^{-2}$ |
| $T_{dry}$ | Value of *Soil Mois* index, below which *Pred Veg Type* is heath | 2.5 |
| $T_{wet}$ | Value of *Soil Mois* index, above which *Pred Veg Type* is riparian | 65.0 |
| *Vasc AGB* | Vascular plants aboveground biomass | $g m^{-2}$ |
| *Vasc Biom* | Above- and belowground biomass of vascular plants | $g m^{-2}$ |
| *Vasc Cover* | Vascular plant cover | - |
| *Vasc Prod* | Vascular plant productivity | $g m^{-2}$ year$^{-1}$ |
| $W_N$ | Effect of *Soil Mois* and *Discharge* on *N Avail* (Fig. 18.3) | 0–1 |

where $S_{min}$ and $D_{min}$ are parameters as shown in Fig. 18.2. Thus, soil moisture is high if discharge is high or if the slope is low; soil moisture is low if the amount of water routed through a site is low or the slope is steep.

### 18.3.1.2 T-VEG

T-VEG is similar to the model of Ostendorf and Reynolds (1996; Sect. 14.4.2; Sect. 17.3.1, this Vol.) and predicts vegetation types based on thresholds of *Soil Mois*:

$$\text{Pred Veg Type} = \begin{cases} \text{Heath} & \text{if Soil Mois} < T_{dry} \\ \text{Riparian} & \text{if Soil Mois} > T_{wet} \\ \text{Tussock tundra} & \text{otherwise,} \end{cases} \quad (3)$$

where $T_{dry}$ and $T_{wet}$ are thresholds such that the heath vegetation type is assumed to occur in sites with low soil moisture, the riparian vegetation type on sites with high moisture, and tussock tundra with intermediate moisture.

### 18.3.1.3 T-NUT

T-NUT computes N availability (*N Avail*), which is assumed to increase with increasing soil moisture, up to a maximum level. Beyond this maximum additional soil moisture is assumed to lead to saturated, anaerobic soils with a subsequent reduction in *N Avail*. This reduction is ameliorated by high discharge, i.e., increased soil aeration when large amounts of water are routed

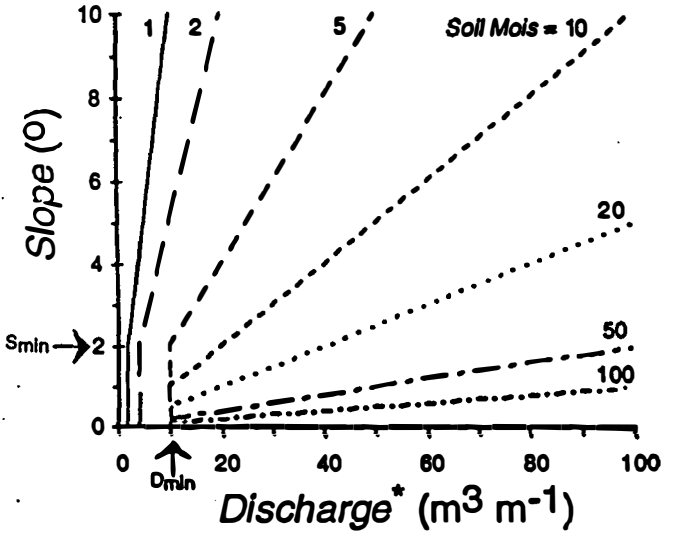


Fig.18.2 *Soil Mois* as a function of *Slope* and *Discharge*

through a site. We compute two scalars, $M_N$ and $W_N$, that reduce *N Avail* from a maximum based on the relative values of *Soil Mois* and *Discharge**, respectively:

$$N\,Avail = N_{max} \cdot (M_N + W_N). \tag{4}$$

$M_N$ and $W_N$ are illustrated in Fig. 18.3, where $M_N^{min}$ is the minimum allowable value of $M_N$.

### 18.3.1.4 T-PLT

T-PLT computes productivity and biomass for the three functional groups of plants, i.e., lichens, mosses, and vascular plants. In contrast to T-VEG, witch predicts a single vegetation type per pixel Eq. (3), T-PLT computes productivity and biomass for each functional group that may occur in a given pixel. Scalars, with values that range from 0 to 1, are used to represent the effect of soil moisture ($M_k^i$), vascular plant shading ($S_k^i$), and dust ($D_k^i$) on process *i* in functional group *k*.

The productivity equations are given by:

$$Vasc\,Prod = NUE \cdot N\,Avail \tag{5}$$

$$Moss\,Prod = Moss\,Biom \cdot PB_{Moss} \cdot S_{Moss}^{Prod} \tag{6}$$

$$Lichen\,Prod = Lichen\,Biom \cdot PB_{Lichen} \tag{7}$$

Vascular plant productivity is assumed to be directly proportional to *N Avail* via a nitrogen use efficiency (NUE). Moss and lichen productivities are

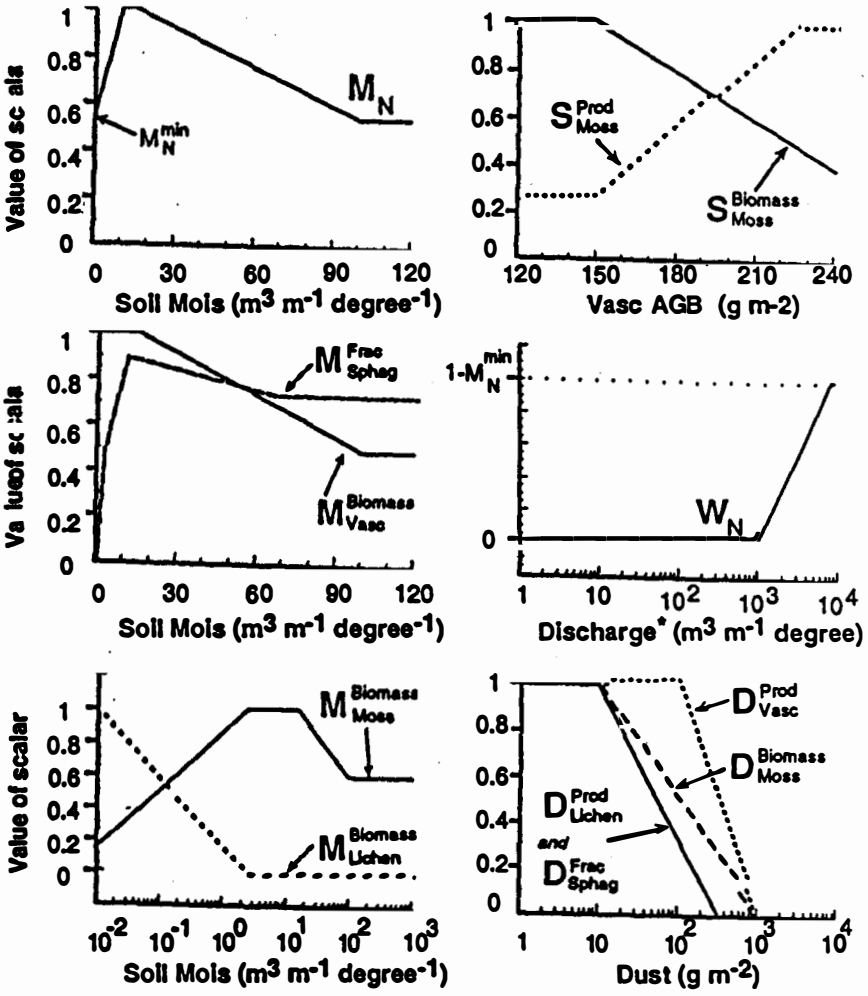


Fig.18.3 Scalars used in T-MAP. (See Table 18.1 for definitions)

computed as functions of total biomass (see below) and productivity: biomass ratios ($PB_k$). The moss productivity: biomass ratio varies as a function of vascular aboveground biomass via the shading scalar, $S^{Prod}_{Moss}$ (Fig. 18.3), which represents increased moss productivity with increasing shading by vascular plants.

The biomass equations are given by:

$$Vasc\ Biomass = Vasc\ Prod\ /\ (PB_{Vasc} \cdot M^{Biomass}_{Vasc}) \quad (8)$$

$$Moss\ Biom = Moss\ Biom\ Max \cdot M^{Biomass}_{Moss} \cdot S^{Biomass}_{Moss} \quad (9)$$

$$Lichen\ Biom = Lichen\ Biom\ Max \cdot M^{Biomass}_{Lichen} \quad (10)$$

For vascular plants, biomass is a function of a productivity: biomass ratio, which varies according to a soil moisture scalar, $M^{Biomass}_{Vasc}$, i.e., productivity: biomass ratios are highest on moist sites (Fig. 18.3). Vascular aboveground biomass (*Vasc AGB*) is calculated from $PB_{Vasc}$:

$$Vasc\ AGB = Vasc\ Prod/PB_{Vasc}. \quad (11)$$

Moss and lichen biomass are computed by adjusting a maximum potential biomass (representing optimum conditions) by moisture scalars. For mosses, as *Soil Mois* increases between 0 and 5, there is a sharp increase in $M^{Biomass}_{Moss}$ to a value of 1 (optimum moisture conditions), which is maintained up to a *Soil Mois* of ca. 15. Moss biomass is also affected by the aboveground vascular plant biomass: as *Vasc AGB* increases, $S^{Biomass}_{Moss}$ decreases reflecting the negative effects of shading (Fig. 18.3).

Total aboveground biomass (*TAGB*) is:

$$TAGB = Vasc\ AGB + Moss\ Biom + Lichen\ Biom, \quad (12)$$

and from Eqs. (5–7) net primary productivity (*NPP*) is:

$$NPP = Vasc\ Prod + Moss\ Prod + Lichen\ Prod. \quad (13)$$

The following sources were used to parameterize T-PLT: Tenhunen et al. (1992) and Oberbauer et al. (Chap. 11, this Vol.) for vascular plant, moss, and lichen biomass at Imnavait Creek and Eagle Creek (south of the Brooks Mountains); Tenhunen et al. (1992) for general patterns of arctic moss productivity; Shaver and Chapin (1991) and Chapter 5 (this Vol.) for vascular plant, moss, and lichen biomass, productivity, and NUE at various sites near Imnavait Creek; and Chapin (1989) for NUE in arctic vascular plants. Shaver and Chapin (1991) found that NUE, measured as the N in annual biomass production, is nearly constant over many types of arctic ecosystem, and that productivity: biomass ratios for arctic plants were the highest in moist vegetation (0.25:1), intermediate in dry vegetation (0.18:1), and lowest in wet vegetation (0.12:1).

### 18.3.2 Disturbance Scenarios

The effects of two categories of road-related disturbances are considered: (1) changes in patterns of water discharge, which modify vegetation and potential for thermokarst erosion, and (2) dust deposition, which has a direct impact on plant biomass and productivity. Simulation results are presented for four differing placements of roads through the watershed as described in Table 18.2.

#### 18.3.2.1 Effects of Altering Discharge

The construction of a road may alter natural patterns of water drainage, effectively acting as a dam. The modification of soil moisture may severely impact

Table 18.2. Characteristics of four simulated roads through the Imnavait Creek watershed

| Road no. | Relative to Imnavait Creek | Length (number of pixels) | Number of culverts | Communities impacted[a] | Compass direction |
|---|---|---|---|---|---|
| 1 | Parallel | 145 | 5[b] | Footslope only | S to N, E side of creek |
| 2 | Parallel | 133 | 0 | Crest only | S to N, E side of creek |
| 3 | Perpendicular | 56 | 1 | All | SW to NE; crosses creek near N end of watershed |
| 4 | Perpendicular | 52 | 1 | All | SW to NE; crosses creek near S end of watershed |

[a]See toposequence of Walker (Fig. 4.8 in Chap. 4, this Vol.).
[b]One at each end of the road and three in areas of high discharge. The elevation map was altered to allow water to flow freely along the road to the culverts.

vegetation at both the patch and landscape scales and over the short and long term. T-MAP allows us to compare predicted vegetation distribution, biomass, and production before and after road building, assuming long-term equilibration has occurred.

### 18.3.2.2 Effects of Road Dust

Dust loads in the vicinity of the road were simulated based on the observations made by Walker and Everett (1987) near Imnavait Creek during 1978, and are similar to the model output from Lamprecht and Graber (Chap. 15, this Vol.). The following approximation to the dust model results was used:

$$Dust\ Load = \begin{cases} D_{max} & \text{if } Dist < 8 \\ D_{max}/(Dist - 7) + \text{Random} & \text{otherwise,} \end{cases} \quad (14)$$

where *Dist* is distance from the road, $D_{max}$ is the maximum dust load, and Random is random variance.

The most detrimental effects of road dust are on lichens and *Sphagnum* species (Walker and Everett 1987; Chap. 4, this Vol.). Some non-*Sphagnum* mosses and some lichens may actually benefit from dust damage to other nonvascular species. Four scalars were used to represent the effect of dust on vascular productivity ($D_{Vasc}^{Prod}$), moss biomass ($D_{Moss}^{Biomass}$), fraction *Sphagnum* biomass ($D_{Sphag}^{Frac}$), and lichen biomass ($D_{Lichen}^{Biomass}$). These dust scalars are illustrated in Fig. 18.3 and are based on the work of Walker and Everett (1987), Meininger and Spatt (1988), and Santelmann and Gorham (1988).

The effects of dust on the productivity and biomass of the functional groups are given by:

$$Vasc\ Prod = \mathrm{NUE} \cdot N\ Avail \cdot D_{Vasc}^{Prod} \tag{15}$$

$$Moss\ Biom = Moss\ Biom\ Max \cdot M_{Moss}^{Biomass} \cdot S_{Moss}^{Biomass} \cdot D_{Moss}^{Biomass} \tag{16}$$

$$Moss\ Biom\ Sphag = Moss\ Biom \cdot M_{Sphag}^{Frac} \cdot D_{Sphag}^{Frac} \tag{17}$$

$$Lichen\ Biom = Lichen\ Biom\ Max \cdot M_{Lichen}^{Biomass} \cdot D_{Lichen}^{Biomass} \tag{18}$$

In Eq. (17) we assume that the fraction of moss biomass and productivity attributable to *Sphagnum* moss species (i.e., $M_{Sphag}^{Frac}$) peaks at moderate moisture and declines with increasing moisture.

### 18.3.3 Model Validation and Limitations

It is not possible to validate T-MAP directly at the present time. However, we compared output from T-MAP to a satellite-derived map of normalized difference vegetation index (NDVI, derived from a SPOT/HRV-XS scene, June 22, 1987; Stow et al. 1989) and to a map of observed vegetation types (Walker et al. 1989) for the Imnavait Creek watershed. These observed data sets are referred to as *Obs NDVI* and *Obs Veg Type*, respectively. The remotely sensed NDVI is linearly related to the amount of photosynthetically active radiation (PAR) intercepted by vegetation in other systems (Hatfield et al. 1984; Seller 1987). NDVI may provide a measure of net primary productivity, because there is a close relationship between integrated intercepted PAR and NPP in many types of vegetation (Monteith 1981).

## 18.4 Model Predictions for Undisturbed Watershed

The dominant features of the Imnavait Creek watershed are apparent in the maps of *Obs Veg Type* and *Obs NDVI* (Fig. 18.4). Both the dry heath vegetation on the ridges and the wet riparian vegetation in the basin of the watershed are characterized by a low NDVI. Higher values of NDVI delimit the slopes with tussock tundra. The extent of the southwest facing (eastern) slope contrasts strongly with that of the steep northeast facing (western) slope. The eastern slope has numerous well-developed water tracks (Fig. 18.4), which are associated with high *Obs NDVI* (Stow et al. 1989). Within a class of *Obs Veg Type*, we suspect that leaf area index is probably directly proportional *Obs NDVI*, but this has not been validated (cf. Chap. 7, this Vol.).

### 18.4.1 Vegetation

The spatial agreement between *Pred Veg Type* determined with T-VEG and *Obs Veg Type* in the watershed was ca. 76% (Table 18.3; Fig. 18.4). T-VEG is most

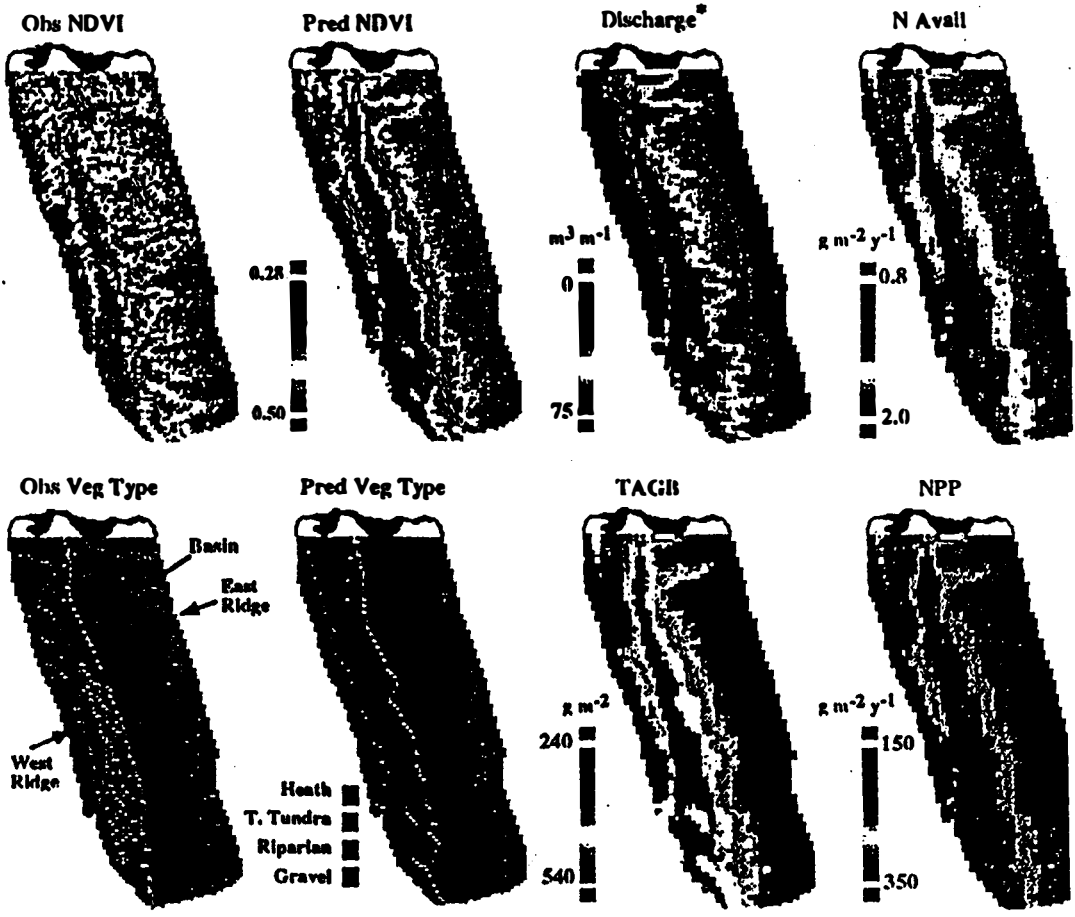


**Fig.18.4 Observed NDVI and vegetation in Imnavait Creek watershed compared with predicted variables from T-MAP**

**Table 18.3.** Comparison of *Obs Veg* and *Pred Veg* maps in the Imnavait Creek watershed

| | Number of map pixels | | |
|---|---|---|---|
| Vegetation types | *Obs Veg*[a] | *Pred Veg* | % Matching |
| Dry heath | 950 | 1053 | 68.0 |
| Tussock tundra | 3533 | 3128 | 77.5 |
| Riparian | 549 | 851 | 79.0 |
| Total | 5032 | 5032 | 75.9 |
| Evenness index | 0.56 | 0.71 | |
| Contagion index | 0.36 | 0.37 | |

[a] Aquatic and barren types (a total of 13 pixels) were assigned to wet and moist types, respectively, because they are not included in

successful (ca. 80%) in predicting the distribution of tussock tundra and riparian types, whereas community distribution on the ridges is reproduced at ca. 68%. The success of the model is due partly to the strong relationships of vegetation to some environmental variables (e.g., moisture and slope), and partly to the aggregation of vegetation into the three functional groups. For example, vegetation in the basin is a mosaic of wet and moist vegetation types (Chap. 4, this Vol.). The transitions between community types depend on microtopographic variation at a scale much finer than is described by T-HYDRO. The results of vegetation mapping presented here are slightly different from those presented in Fig. 17.3 of Ostendorf et al. (Chap. 17, this Vol.) because of small differences in threshold values (heath is restricted solely to dry types and does not include moist CDS heath; see Chap. 5, this Vol.) and as a result of including $S_{min}$ and $D_{min}$.

Two landscape indices, evenness and contagion, were used to compare the *Obs Veg Type* and the *Pred Veg Type* maps. Evenness index represents changes in proportions of the three vegetation types (Romme 1982), whereas contagion represents neighborhood information. i.e., spatial patterns of vegetation distribution (Li and Reynolds 1993). The higher value of evenness for the predicted map reflects the changes of the proportions caused by the prediction errors (Table 18.3). However, the same prediction errors resulted in only a small change in contagion. These indices suggest that, although T-VEG may not get the exact proportions of the cover types and the exact locations of all pixels, it does preserve spatial pattern of the vegetation distribution.

### 18.4.2 Discharge

Annual *Discharge** is strongly correlated with many of the dominant features of the watershed as evident in the map produced by T-HYDRO (Fig. 18.4). The ridge tops are characterized by low discharge and the basin by very high discharge. Water track channels in the Imnavait Creek catchment are ca. 5–20 m wide and are depressed ca. 0.25–1 m in relation to adjacent tussock tundra (Hastings et al. 1989; Chap. 4, this Vol.). The most prominent water track in the watershed (water track 3, Fig. 9.2, this Vol.) is on the northern end of the eastern slope, which shows up as an area of high *Discharge** (Fig. 18.4). Other areas of high *Discharge** on the eastern slope, i.e., the patterning with a series of stripes with high discharge, also correspond to areas with well-developed water tracks. *Soil Mois* and *Discharge** have nearly identical patterns for the ridges and slopes, but due to a rapid decrease in *Slope*, *Soil Mois* increases much more rapidly than *Discharge** at the boundary between the bottom of the slopes and the basin (not shown).

### 18.4.3 N Availability and NPP

Predicted total aboveground biomass [*TAGB*, Eq. (12)] is highest on the ridges, declines toward the bottoms of the slopes, and is the lowest in the basin (Fig.

18.4). The comparison to actual biomass harvests in the watershed is very good (see Table 5.5, this Vol.). Vascular plant biomass increases from the ridge to the bottom of the slope on both sides of the watershed, lichen biomass decreases to zero within 100 m of the ridges, and moss biomass declines in areas of high discharge, due to high vascular plant biomass (not shown). *N Avail* and *NPP* (Fig. 18.4) are low on the ridges and in the basin, and highest at the bottoms of the slopes and in water tracks. Most of the other variables that are directly related to *NPP*, i.e., vascular plant productivity, moss productivity, and total vascular plant biomass, also follow these patterns.

### 18.4.4 Model Evaluation

Spatial correlations between various output variables of T-MAP and observed NDVI are given in Table 18.4. The correlation between *Discharge** and *Obs NDVI* is poor, because NDVI is low in both the basin and ridges, whereas *Discharge* is high in the basin and low on the ridges. *Soil Mois* is also poorly correlated to NDVI. On the other hand, *N Avail*, which is a function of both *Soil Mois* and *Discharge**, has a much higher correlation with NDVI. The correlation between *TAGB* and *Obs NDVI* is poor, because T-MAP simulates low *TAGB* in areas with the highest NDVI (e.g., at the foot of the eastern slope). This may be part of the reason why NDVI was poorly correlated with leaf area index, total community biomass, and total green biomass in "ground truth" measurements (Chap. 7, this Vol.). It must also be noted that NDVI may be sensitive to aspects of tundra ecosystem structure that have little to do with plant biomass or productivity, e.g., surface water, exposure of mineral soil in the ridge heath, etc. (Sect. 7.3, this Vol.).

*NPP* has the highest correlation ($r = 0.66$) with *Obs NDVI*. Both variables are strongly dependent on community structure. We regressed *NPP* on *Obs*

Table 18.4. Correlation coefficients for comparisons of maps of modeled variables with the *Obs NDVI* map. Resample statistics, which are less influenced by spatial autocorrelations, are based on 50 resamples with $n = 30$ for each sample

| Model output | r | $r^2$ | Resample mean $r^2$ | Resample variance |
|---|---|---|---|---|
| Abiotic variables | | | | |
| *Discharge** | −0.07 | <0.01 | 0.06 | 0.003 |
| *Soil Mois* | −0.13 | 0.02 | 0.08 | 0.005 |
| *Slope* | 0.20 | 0.04 | 0.05 | 0.004 |
| Biotic variables | | | | |
| *N Avail* | 0.65 | 0.42 | 0.43 | 0.006 |
| *Vasc AGB* | 0.65 | 0.42 | 0.43 | 0.012 |
| *Moss Biom* | <0.01 | <0.01 | 0.01 | 0.001 |
| *Lichen Biom* | −0.1 | 0.01 | 0.02 | <0.001 |
| *TAGB* | −0.10 | 0.01 | 0.05 | 0.004 |
| *NPP* | 0.66 | 0.44 | 0.45 | 0.006 |

*NDVI* to obtain a "predicted" NDVI, i.e., *Pred NDVI* = a + b * *NPP*. *Pred NDVI* does not add new information, but instead transforms *NPP* into NDVI units, which allows us to make a better visual comparison with the *Obs NDVI* map (Fig. 18.4). Low *Pred NDVI* occurs on the ridges and in the basin. *Obs NDVI* increases toward the foot of both slopes, and some of this variation along the slope is also apparent in the *Pred NDVI* map. The most highly developed water track in the watershed – a region of high NDVI at the north end of the east slope – is obvious in the *Pred NDVI* map. The primary discrepancies between *Pred NDVI* and *Obs NDVI* are (1) less variation in *Pred NDVI* along the slopes and ridges than in the observed NDVI; (2) a wider and longer area of low *Pred NDVI* in the basin than observed; and (3) a band of low *Pred NDVI* along the west ridge that is much more prominent than observed. These discrepancies may be attributed to inherent limitations in the resolution of the DEM map, the assumption of a uniform water budget, a lack of stochasticity in the hydrology and vegetation models, and other factors not included in the model. Despite these limitations, the *Pred NDVI* predicted by the T-MAP model accounts for 45% of the variation in the *Obs NDVI* (Table 18.4).

## 18.5 Model Predictions for Disturbed Watershed

The predicted changes in vegetation type and biomass presented here must be considered as qualitative measures (relative indicators) of the effects of disturbance on vegetation, rather than quantitative measures (absolute amounts). The response to disturbances is a relatively short-term adjustment, yet the relationships between soil moisture and vegetation pattern and processes upon which T-MAP is based also depend on long-term system evolution. e.g., soil development, population redistribution, snow accumulation patterns, etc., which are not considered. Other limitations are discussed in Section 18.6.3.

### 18.5.1 Discharge Disturbance

The four roads (Table 18.2) alter patterns of discharge by impeding downslope movement of water. The resulting changes in the soil moisture index are input into the T-VEG, T-NUT, and T-PLT models (see Fig. 18.1). The predicted changes in ecosystem structure and function in response to disturbance are summarized in Figs. 18.5 and 18.6, and in Table 18.5. While altered spatial patterns are found for all the variables discussed previously, predicted changes in biomass are emphasized.

#### 18.5.1.1 Road #1

Water moves down the eastern slope until it is blocked by the road. It is then [illegible] the culverts where it again moves downslope (Fig.

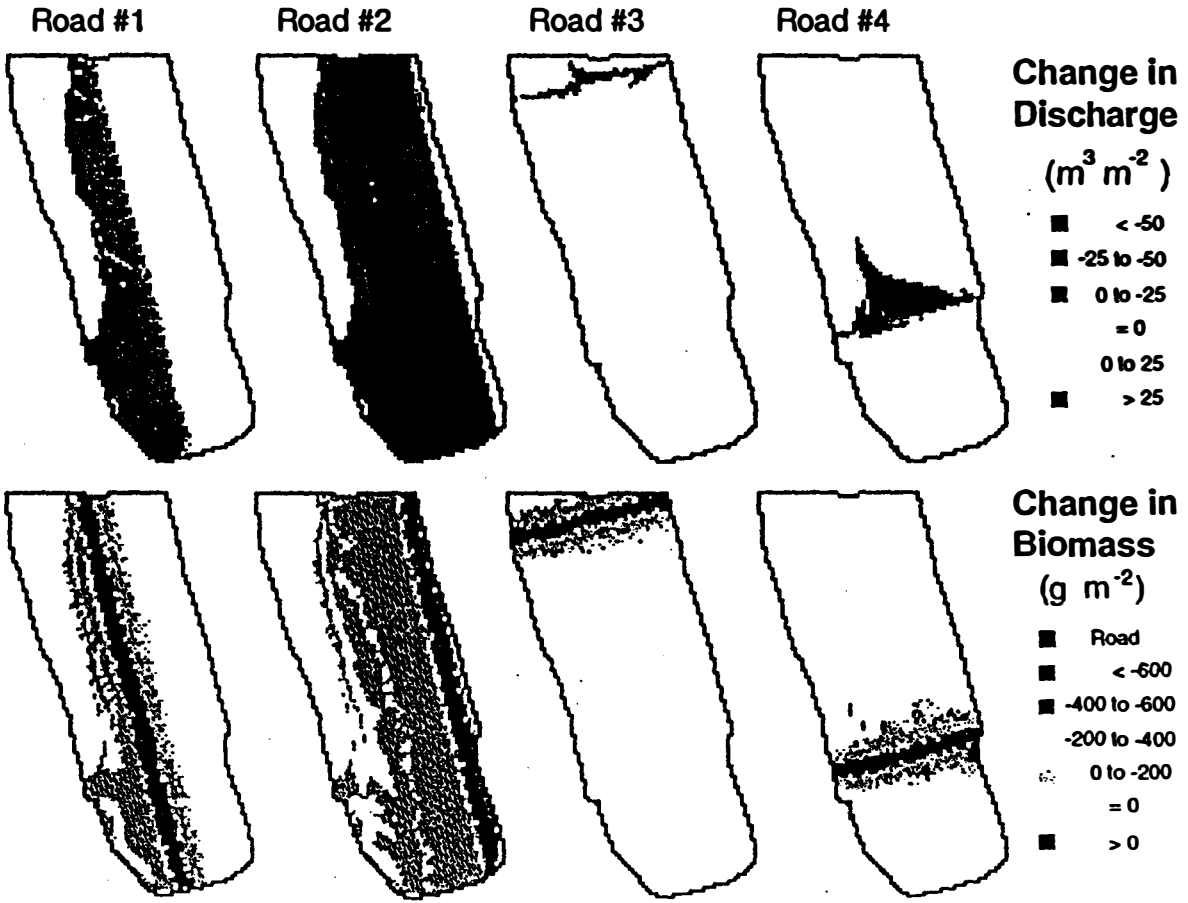


Fig.18.5 Simulated changes in discharge and total aboveground biomass caused by the construction of four roads through the watershed

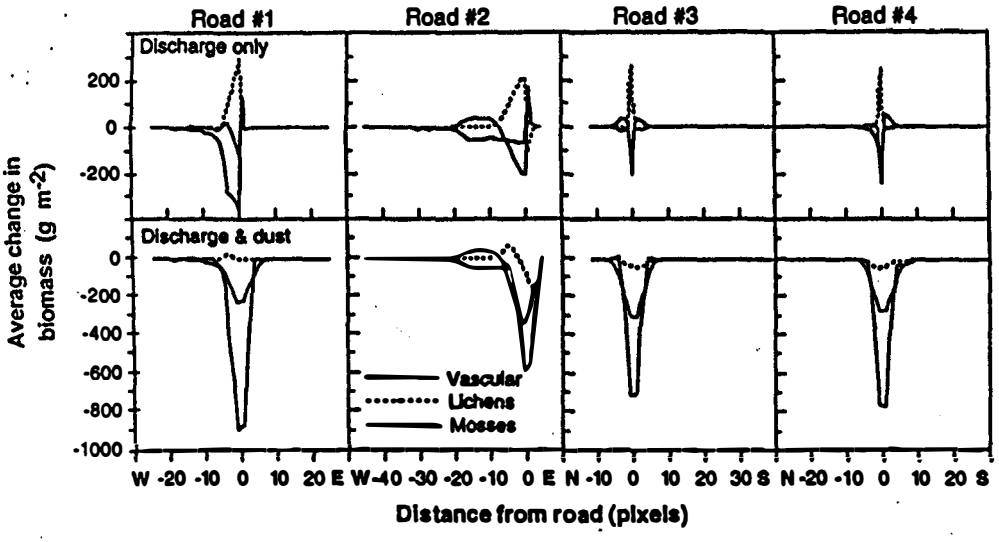


Fig.18.6 Simulated average changes in discharge and aboveground biomass of three functional plant types as a function of distance from the four roads

18.5). This leads to high values of *Discharge** immediately above the road and a consequent increase in vascular plant biomass. In areas immediately west and downslope from the road, there is a large decrease in water discharge. These changes in discharge result in a substantial decrease in vascular plant and moss biomass. There is also a large change in the fraction of *Sphagnum* moss predicted for this area (not shown). Under this scenario the change in soil moisture may be profound enough to cause extensive death to existing vegetation. Lichen biomass is predicted to increase in the areas immediately below the road; yet the rate at which lichens might exploit such new favorable habitat is likely to be very slow. As Walker (Chap. 3, this Vol.) points out, many construction areas that create dry habitat remain free of vegetation for long periods, even when artificial revegetation is attempted. Overall, the construction of road #1 is predicted to decrease plant biomass ca. 15.9 kg $m^{-1}$ road, with vascular plant biomass being most negatively affected (Table 18.5). High soil moisture predicted for areas originally covered with *Sphagnum* may indicate that altered discharge may cause melting of ground ice and severe thermokarst erosion (Chap. 3, this Vol.). Further downslope, discharge from the culverts fans out and the effects on vegetation decrease substantially (Figs. 18.5 and 18.6).

### 18.5.1.2 Road #2

This road is placed high enough on the east ridge so that relatively little water

Table 18.5. Predicted changes in biomass and percentage of watershed affected for the three plant functional types in the Imnavait Creek watershed resulting from the construction of four roads (see Table 18.2). Statistics are for percentages of watershed affected

| | Road no.1 (145 pixels) | | Road no.2 (133 pixels) | | Road no.3 (56 pixels) | | Road no.4 (52 pixels) | |
|---|---|---|---|---|---|---|---|---|
| **Changes in discharge only** | | | | | | | | |
| **Vascular Plants** | | | | | | | | |
| Mean increase (kg/pixel[a]) | 34.2 | 4%[b] | 52.9 | 3% | 13.0 | 7% | 9.7 | 5% |
| Mean decrease (kg/pixel) | −69.4 | 24% | −16.1 | 63% | −41.3 | 2% | −35.6 | 5% |
| Net change (kg biomass/m of road length[c]) | −26.3 | | −16.4 | | −0.6 | | −5.8 | |
| **Lichens** | | | | | | | | |
| Mean increase (kg/pixel) | 85.7 | 9% | 53.8 | 17% | 93.0 | 1% | 76.2 | 2% |
| Mean decrease (kg/pixel) | 0.0 | 0% | −35.9 | 3% | −14.0 | 1% | −8.4 | 2% |
| Net change (kg biomass/m of road length) | 14.1 | | 15.8 | | 4.8 | | 5.3 | |
| **Mosses** | | | | | | | | |
| Mean increase (kg/pixel) | 12.3 | 11% | 12.7 | 35% | 8.2 | 2% | 7.9 | 4% |
| Mean decrease (kg/pixel) | −21.5 | 16% | −30.5 | 31% | −22.1 | 6% | −22.0 | 5% |
| Net change (kg biomass/m of road length) | −3.7 | | −9.5 | | −5.5 | | −3.7 | |
| Total net change (kg biomass/m road length) | −15.9 | | −10.1 | | −1.3 | | −4.2 | |
| **Vascular Plants** | | | | | | | | |
| Mean increase (kg/pixel) | 10.0 | 1% | 0.0 | 0% | 6.2 | 4% | 2.5 | 3% |
| Mean decrease (kg/pixel) | −157.0 | 30% | −46.0 | 67% | −210.4 | 6% | −172.5 | 8% |
| Net change (kg biomass/m of road length) | −80.6 | | −58.7 | | −53.1 | | −63.4 | |
| **Lichens** | | | | | | | | |
| Mean increase (kg/pixel) | 15.6 | 3% | 22.0 | 10% | 0.0 | 0% | 2.4 | 0% |
| Mean decrease (kg/pixel) | 0.0 | 0% | −47.1 | 10% | −52.2 | 2% | −33.3 | 4% |
| Net change (kg biomass/m of road length) | 0.8 | | −4.7 | | −4.3 | | −5.7 | |
| **Mosses** | | | | | | | | |
| Mean increase (kg/pixel) | 8.6 | 5% | 11.9 | 31% | 0.4 | 0% | 1.6 | 1% |
| Mean decrease (kg/pixel) | −45.2 | 34% | −53.1 | 36% | −61.6 | 12% | −54.1 | 12% |
| Net change (kg biomass/m of road length) | −26.2 | | −28.9 | | −32.0 | | −32.4 | |
| Total net change (kg biomass/m road length) | −106.0 | | −92.2 | | −89.4 | | −101.5 | |

[a] Pixel = 20m × 20m.
[b] Based on a total of 5032 pixels in watershed.
[c] Length of road = no. pixels × 20m.

an area where small changes in soil moisture have relatively large impacts on the lichens and mosses. Overall, road #2 is predicted to decrease plant biomass ca. 10.1 kg $m^{-1}$ road (Table 18.5). Areas immediately downslope from the road become drier resulting in a decline in moss biomass, an increase in lichen biomass, and a slight decline in vascular plant biomass (initially low due to dry conditions). The prediction of short-term increases in lichen biomass seems more likely in this scenario compared with that for road #1, because the affected areas are in (or near) areas with high initial lichen biomass. Changes in biomass propagate much further downslope than for road #1 (see number of pixels affected in Table 18.5).

#### 18.5.1.3 Roads #3 and #4

These roads are perpendicular to the elevation contours with culverts placed at the lowest elevation. Therefore, the downslope movement of water is not impeded. Consequently, only small areas on either side of the roads are affected. Large changes in biomass occur only in the immediate vicinity of the roads, and in pixels where localized damming or drying occurs. Road #4 results in greater biomass changes than road #3 (Table 18.5), because the orientation is not exactly perpendicular to the elevation contours. The most likely negative effect of these roads would be damage due to melting of massive ground ice and thermokarst erosion immediately adjacent to the road in the basin of the watershed where soil moisture and *Sphagnum* moss biomass are high.

### 18.5.2 Dust and Discharge Disturbance

Dust combined with discharge disturbance is predicted to cause substantially greater changes in vascular plant and moss biomass than discharge disturbance alone (Fig. 18.6). The predicted net loss of biomass per meter of road is roughly the same in all scenarios when dust and discharge effects are combined, ca. 90–110 kg (Table 18.5). There are, however, relatively large differences in how this change is distributed among functional groups.

Road #1 has relatively large effects on vascular plant biomass, because this road passes through communities with high vascular plant biomass. In contrast, there is minimal effect on lichens as they are not predicted to occur in the neighborhood of this road. Road #2 has larger negative and positive effects on lichens (see number of pixels affected, Table 18.5), because this road passes through areas with high lichen biomass. Some damage occurs in an adjacent watershed that is not included in the analysis. Roads #3 and #4 pass through all vegetation types and, therefore, change biomass of all functional groups. In all scenarios, the order in which biomass is negatively affected is: vascular plants > mosses > lichens

### 18.5.3 Effect of Disturbance on Spatial patterns

For both the undisturbed and disturbed watershed (the four road scenarios with both discharge and dust) we constructed omnidirectional (i.e., average of all directions) and directional (N15°W and N75°E) semivariograms for all variables (abiotic and biotic). Semivariograms, which relate variation to scales, are useful tools to depict and analyze spatial patterns (Fortin et al. 1989; Rossi et al. 1992). The directional semivariograms coincide with the major environmental gradients in the watershed, i.e., N75°E is perpendicular to the creek and N15°W is parallel to the creek. Only the results for biomass of the three

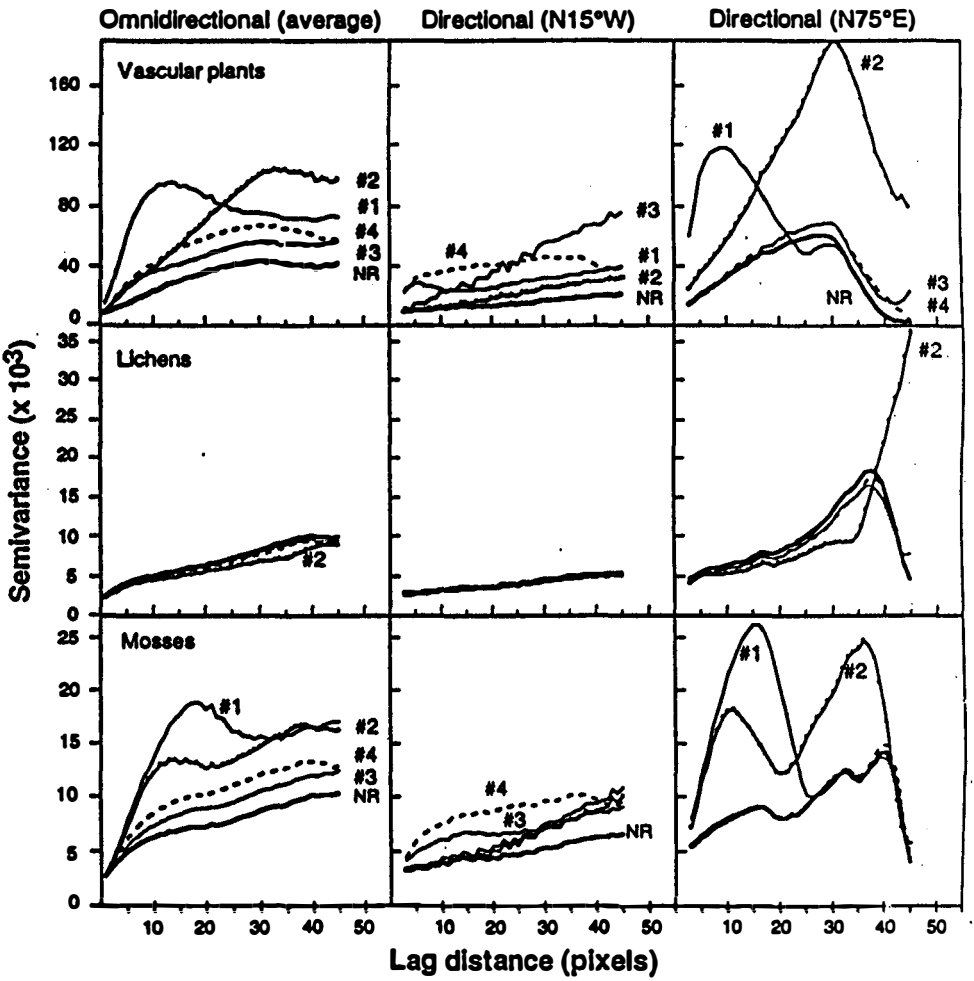


Fig.18.7 Omnidirectional and directional semivariograms of biomass of the three functional groups under four road scenarios (see Table 18.2). NR = no road

functional types of plants are described here (see Chap. 14, this Vol. for other variables). The semivariograms without road disturbance depict the background variation of plant biomass in the watershed. Of course, the general shape of the semivariograms is to a great extent controlled by spatial patterns of the driving variables in T-MAP (e.g., discharge, soil moisture, and nutrient availability).

The semivariogram analysis show that different road scenarios exert distinct effects on biomass distribution of the three functional groups (Fig. 18.7) Firstly, the omnidirectional semivariograms indicate that roads #1 and #2 generally cause more changes in spatial variations of biomass than roads #3 and #4. Secondly, the directions of the roads produced different effects. In the N75°E direction biomass distributions change greatly with roads #1 and #2, but little with roads #3 and #4, because the former enhance/magnify the gradients in this direction. Biomass distributions change with all four roads in the N15°W direction. Thirdly, the location of roads in the same direction also makes large differences in changes in spatial distribution of biomass. Road #1 changes the shape of the semivariogram in the N75°E direction, producing a profound peak of variation at a small scale (i.e., about the lag distance of 10 pixels). In contrast, road #2 shows a predominant peak in the N75°E direction at a large scale (30 pixels), which coincides with the peak in the semivariogram without roads. In addition, road #2 causes the only significant change in spatial variations of lichen biomass in the N75°E direction. This is because road #2 is along the ridge tops where lichens predominate in the dry heath communities. Fourthly, the three functional groups are affected differently. Spatial variations of biomass of vascular plants and mosses show significant changes in both directions examined, but those of lichens display little change, except for the one caused by road #2 in the N75°E direction. This difference among the three functional groups is likely due to both their distributions in the watershed and to their differential responses to dust and discharge changes.

## 18.6 Discussion

### 18.6.1 Model Comparisons

Several other groups have used simple water-routing routines to predict vegetation properties and have had varying success. For example, Costanza et al. (1990) successfully used an empirical water routing routine to simulate the response of vegetation in the Mississippi river delta to changes in water management. Brown (1994) used upslope drainage area and slope to predict soil moisture using an algorithm similar to the one used here. Brown coupled this soil moisture index with elevation, potential insolation index, and a snow potential index to predict alpine vegetation types in Glacier National Park. He was able to explain only about 38% of the variation in vegetation type. The

success of our approach and that of Costanza et al. probably lies in the importance of water in determining vegetation type in these ecosystems, and in the lack of deep seepage of water.

T-MAP builds on the discharge models developed by Ostendorf and Reynolds (1993 and Chaps. 14 and 17, this Vol.), and integrates hydrological perspectives with an ecosystem model. Whereas Ostendorf and Reynolds correlated NDVI with predicted discharge patterns in the Imnavait Creek watershed, added explanation is achieved with T-MAP, because discharge patterns can be related to nutrient and vegetation patterns, which can then be related to remotely sensed NDVI. The patterns of discharge in our model (with the exception of the basin) are similar to those described by Ostendorf and Reynolds who used a 10- × 10-m pixel elevation map. *Discharge** is uniformly high in the basin in our maps and striations of low and high *Discharge** that they reported for their simulations do not occur. With coarser resolution maps there is also a decrease in the definition of water tracks as compared with Ostendorf and Reynolds.

T-MAP improves on the model of Ostendorf and Reynolds by predicting patterns for the entire watershed, not just the ridges and slopes. Ostendorf and Reynolds excluded values of *Discharge** over 60 $m^3 m^{-1}$ (i.e., basin values) in their analysis of the relationship between *Discharge** and observed NDVI. We find a nearly identical relationship when we exclude values of Discharge over 60 $m^3 m^{-1}$ in T-MAP (Fig. 18.8). Inclusion of high *Discharge** values substantially degrades this relationship, because *Obs NDVI* is low on the ridges and in the basin, whereas *Discharge** is low on the ridges and high in the basin. The relationship of *NPP* to *Obs NDVI* is much better than the relationship between *Discharge** and *Obs NDVI* when the entire basin is included in the analysis (Fig. 18.8).

### 18.6.2 Patterns of N Availability

Our predicted patterns of N availability, i.e., high in water tracks, intermediate in moist sites, and low in dry and wet sites, contrast with those measured by Giblin et al. (1991) and reported in Nadelhoffer et al. (1992). In addition, their annual rates of N mineralization for dry and wet vegetation (ca. 0.5 g $m^{-2}$ $year^{-1}$) are considerably lower than our estimates (1.2–1.4 g $m^{-2}$ $year^{-1}$), and they report a rate of N mineralization in tussock tundra (ca. 0.1 g $m^{-2}$ $year^{-1}$) that is more than an order of magnitude lower than our predicted values (1.2–1.6 g $m^{-2}$ $year^{-1}$). There are several lines of evidence that suggest the data of Giblin et al. (1991) may not reflect typical patterns or magnitudes of N availability on tussock-tundra slopes (cf. Chap. 10, this Vol.).

Our estimates of N cycling rates are based on (1) measurements of plant productivity and N use efficiency from a wide variety of North Slope tundra sites, and (2) simulation models of N uptake by arctic tundra plants (Leadley and Reynolds 1992; Leadley et al. 1996, see Chap. 14, this Vol). McGuire et al.

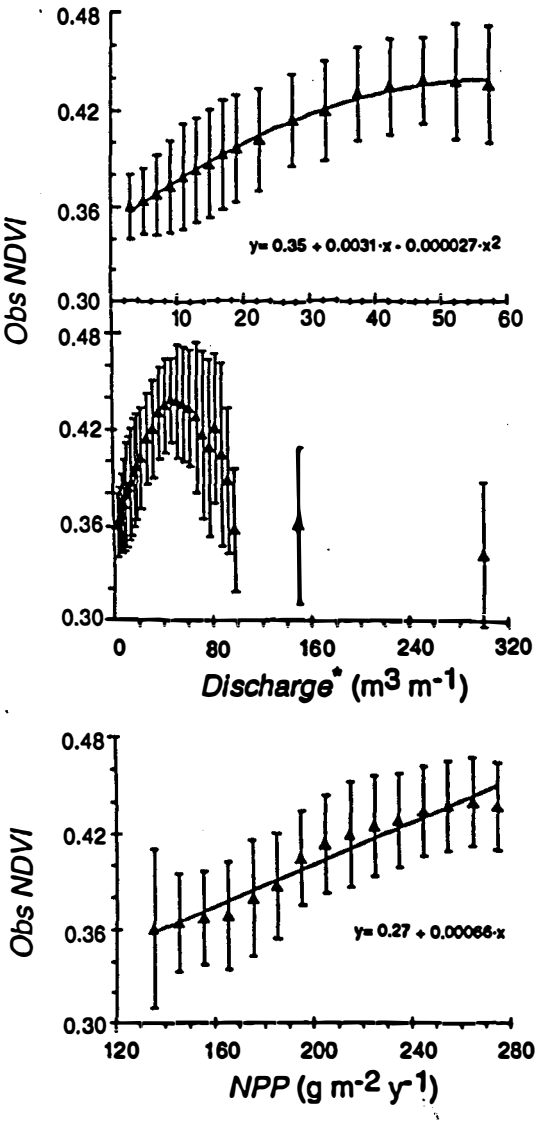


**Fig.18.8** Relationship between *Obs NDVI* and *Discharge** and *NPP*. Values represent the means and standard errors of all values in the map that are equidistant from the *Discharge** value. In *top panel*, analysis is limited to values of *Discharge** less than 60 $m^3 m^{-1}$; in *middle panel*, means were unequally spaced to reduce the number of points on the graph and to roughly equalize the number of pixels represented by each point. Comparisons of variances between unequally spaced points is not appropriate

(1992) found that simulated N mineralization for North American sites overlapped observed N mineralization rates reported in Nadelhoffer et al. (1992) in all ecosystem types except in the Arctic. They found that they needed 0.3–1.43 $g m^{-2} year^{-1}$ of N mineralization to account for plant productivity in wet and moist tundra ecosystems, whereas Nadelhoffer et al. give a range of ca. 0.04–0.5 $g m^{-2} year^{-1}$. Our review of productivity and N-use efficiency by tussock-tundra plants would lead to a value of N availability that is not less than 0.6 $g m^{-2}$ $year^{-1}$ (compared with 0.1 $g m^{-2}$ $year^{-1}$ reported by Giblin et al 1991).

Giblin et al. and Nadelhoffer et al. suggest that uptake of organic N (only inorganic N mineralization rates were measured in their study) may account for the discrepancy between observed plant N uptake and their estimates of net N mineralization. There is evidence for at least one important tussock-tundra species, *Eriophorum vaginatum*, that organic sources of N can account for more than 60% of total N uptake in this species (Chapin et al. 1993; Leadley et al. 1996).

The patterns of N mineralization reported by Giblin et al. do not correspond to other patterns that should be related to N uptake by plants. The pattern of *Obs NDVI* indicates an increase in productivity from dry sites to moist sites. It is unlikely that these patterns in NDVI correspond to the order of magnitude decrease in N mineralization reported by Giblin et al. (1991). We believe that Giblin et al. (1991) found such low mineralization rates in moist tundra because they measured N mineralization in intertussock areas. These intertussock areas are often dominated by mosses that provide a very poor substrate for decomposition. Alternatively, the low rates of mineralization may relate to local substrate conditions (see comments in Chap. 10, this Vol.). Measured and modeled estimates of annual N cycling within tussocks (Chapin et al. 1988; Leadley and Reynolds 1992) are much higher than the estimates of Giblin et al. (1991). There may also be problems in relating N mineralization measurements made with buried bags with N uptake by plants (Binkley and Vitousek 1989).

### 18.6.3 Extrapolation Potential: Some Cautionary Notes

Ostendorf and Reynolds (1996; Chap. 14, this Vol.) show that discharge and slope patterns can be used to explain vegetation type patterns in the Imnavait Creek watershed, and that these relationships also hold outside the watershed. However, they also show that these relationships are poor at tundra sites with glaciation histories that differ from the Imnavait Creek watershed. Thus, the results of our modeling work can be extrapolated beyond the Imnavait Creek watershed, but caution must be used when doing so. As in Ostendorf and Reynolds (1996), T-MAP uses slope and discharge to predict vegetation patterns, but the basis is mechanistic (albeit simple mechanism), rather than correlative per se.

There are several caveats that must be considered before using T-MAP for simulations of ecosystem response in larger areas. Firstly, the magnitude of many parameter values are heavily influenced by data collected at the Imnavait Creek site, one of the most intensively studied tussock-tundra sites in Alaska. Although the structure of the model and the form of the relationships should be applicable to most watersheds in the Brooks Mountain foothills, the parameter settings must be tested before they are applied to other watersheds particularly if the glaciation history is different from that of Imnavait Creek catchment. Secondly, T-MAP does not predict the presence of several impor-

tant vegetation types that occur in the Brooks Mountain foothills, e.g., aquatic or tall shrub communities. Thirdly, model development is hindered by a lack of information about vegetation structure. Labor-intensive harvesting of biomass has generally not been designed to be linked with or to support spatial modeling studies. For example, the areas of low observed NDVI at the south end of the basin (Fig. 18.4) received little attention from researchers at Imnavait Creek. Due to concentrated investment of resources in the study of processes in tussock tundra, the dominant vegetation in this region, we have much less confidence in our predictions of rates of processes and patterns for the riparian basin. Fourthly, the discharge model works best in areas with significant topographic relief. It is not possible to accurately route water in relatively flat areas because of the resolution limits in the elevation data base. Fifthly, the discharge model is parameterized with an estimate of the water budget based on a single year. Given the nature of the model, it would be better if it were parameterized with a long-term average of the annual water budget. Finally, we parameterized the *Pred NDVI* regression model based on a single NDVI scene. It would be preferable to use several scenes of NDVI within a year to obtain a better estimate of intercepted PAR. However, because the patterns of variation in NDVI are of primary concern, and less so the absolute values of NDVI, other mid-season NDVI scenes should provide similar correlations.

## 18.7 Conclusions

Roads that disrupt discharge may cause substantial disturbance to arctic ecosystems (Figs. 18.5 and 18.6). Our simulations suggest that disturbance can be minimized by building roads in areas with the smallest effect on discharge patterns. Roads that ascend and descend slopes perpendicular to elevation contours and roads along ridges (i.e., watershed boundaries) are the least likely to cause vegetation disturbance through altered discharge. Dust from roads will have significant impacts regardless of road location.

T-MAP predicts that on a meter-of-road basis, the severity of changes in discharge on vascular plants is: road #1 > road #2 >> road #4 > road #3 (Table 18.5.). Negative effects on moss biomass, due to changes in discharge, are the most severe in road #2 with little difference among the other three scenarios. Negative effects of changing discharge on lichen biomass are restricted to areas where roads pass along the ridges, so the severity of effects is: road #2 > roads #3 and #4 >> road #1. The likelihood of large-scale thermokarst erosion based on *Sphagnum* moss distributions and changes in soil moisture from the most severe to least severe is: road #1 >> road #3 and #4 >> road #2. Dust effects are similar for all roads when all vegetation types are taken into account, but road #2 has greater negative effects on mosses and lichens, and Road #1 has proportionally greater negative effects on vascular plants.

Our conclusions and recommendations based on simulations with T-MAP are:

1. Any road construction has the potential to substantially alter vegetation biomass and community structure over large areas of the watershed. The net change in vegetation biomass and productivity is likely to be large and negative.
2. Roads through the basins of watersheds (e.g., road #1) should be avoided because of the potential for severe discharge-related damage to vascular plant and moss communities, and the potential for widespread thermokarst erosion.
3. Roads along ridges (e.g., road #2) may cause severe damage to lichens and mosses, and the effects of these roads propagate over large areas of the watershed and probably should also be avoided.
4. Roads placed perpendicular to the elevation contours (e.g., roads #3 and #4) are likely to cause the least damage, but these roads disturb small areas of the watershed that are likely to be susceptible to thermokarst erosion.

We show that a model based solely on elevation data and annual water budget can predict the major vegetation types in an arctic watershed (76% success). Furthermore, predictions of net primary productivity can explain ca. 45% of the variation in observed NDVI. Attempts to find direct correlations between ecosystem properties and remotely sensed data often fail. Our approach demonstrates how a simulation model can be used to relate remotely sensed vegetation indices to a wide range of important ecosystem properties, and has potential to become an applied management tool with further development and testing. Such models may serve as valuable tools for generating maps of risk potential of arctic landscapes to various types of disturbances.

*Acknowledgements.* We thank F. S. Chapin III for helpful comments on the manuscript, and A. Hope, D. Stow, and D. A. Walker for helpful discussions of their data. Financial support was provided by NASA Global Change Fellowship program (to P. Leadley) and the US Dept. of Energy (grant nos. DE-FG03-84R60250 and DE-FG05-92ER61455).

## References

Binkley D, Vitousek P (1989) Soil nutrient availability In: Pearcy RW, Ehleringer J, Monney HA, Rundel PW (eds) Plant physiological ecology: field methods and instrumentation. Chapman and Hall, London, pp 75–96

Bonan GB (1993) Do biophysics and physiology matter in ecosystem models? Climate Change 24: 281–285

Brown DG (1994) Predicting vegetation types at treeline using topography and biophysical distubance variables. J Veg Sci 5: 641–656

Burt TP, Butcher DP (1985) Topographic controls of soil moisture distributions. J Soil sci 36: 469–486

Chapin FS III (1989) The cost of tundra plant structures: evaluation of concepts and currencies. Am Nat 133: 1–19

Chapin FS III, Fetcher N, Kielland K, Everett K, Linkins AE (1988) Productivity and nutrient cycling of Alaskan tundra: enhancement by flowing soil water. Ecology 69: 693–702

Chapin FS III, Moilanen L, Kielland K (1993) Preferential use of organic nitrogen for growth by a non-mycorrhizal arctic sedge. Nature 361: 150–153

Costanza R, Sklar FH, White ML (1990) Modeling coastal landscape dynamics. BioScience 40: 91–107

DeAngelis DL, White PS (1994) Ecosystems as products of spatially and temporally varying forces, ecological processes, and landscapes: a theoretical perspective. In: Davis SM, Ogden JC (eds) Everglades: the ecosystem and its restoration. St Lucie Press, Delray Beach, pp 9–27

Fortin M-J, Drapeau P, Legendre P (1989) Spatial autocorrelation and sampling design in plant ecology. Vegetatio 83: 209–222

Giblin, AE, Nadelhoffer K, Shaver GR, Laundre JA, McKerrow AJ (1991) Biogeochemical diversity along a riverside toposequence in arctic Alaska. Ecol Monogr 61: 415–435

Harley PC, Tenhunen JD, Murray KJ, Beyers J (1989) Irradiance and temperature effects on photosynthesis of tussock tundra *Sphagnum* mosses from the foothills of the Philip Smith Mountains, Alaska. Oecologia 79: 251–259

Hastings SJ, Luchessa SA, Oechel W, Tenhunen JD (1989) Standing biomass and production in water drainages of the foothills of the Philip Smith Mountains, Alaska. Holarct Ecol 12: 304–311

Hatfield JL, Asrar G, Kanemasu ET (1984) Intercepted photosynthetically active radiation estimated by spectral reflectance. Remote Sens Envir on 14: 65–75

Kielland K, Chapin FS III (1992) Nutrient absorption and accumulation in arctic plants. In: Chapin FS III, Jefferies RL, Reynolds JF, Shaver GR, Svoboda J (eds) Arctic ecosystems in a changing climate: an ecophysiological perspective. Academic Press, San Diego, pp 321–336

Leadley PW, Reymolds JF (1992) Long-term response of an arctic sedge to climate change: a simulation study. Ecol Appl 2: 323–340

Leadley PW, Reynolds JF, Chapin FS III (1996) A model of ammonium, nitrate, and glycine uptake by *Eriophorum vaginatum* roots in the field: ecological implications (submitted)

Li H, Reynolds JF (1993) A new contagion index to quantify spatial patterns of landscapes. Landscape Ecol 8(3): 155–162

Li H, Reynolds JF (1995) On definition and quantification of heterogeneity. Oikos 73(2): 280–284

McGuire AD, Melillo JM, Joyce LA, Kicklighter DW, Grace AL, Moore B III, Vorosmarty CJ (1992) Interactions between carbon and nitrogen dynamics in estimating net primary productivity for potential vegetation in North America. Global Biogeochem Cycles 6: 101–124

Meininger CA, Spatt CD (1988) Variations of tardigrade assemblages in dust-impacted arctic mosses. Arct Alp Res 20: 24–30

Monteith JL (1981) Does light limit crop production? In: Johnson CB (ed) Physiological processes limiting plant productivity, Butterworths, London, pp 23–38

Murray KJ, Tenhunen JD, Kummerow J (1989) Limitations on moss growth and net primary production in tussock tundra areas of the foothills of the Philip Smith Mountains, Alaska. Oecologia 20: 256–262

Nadelhoffer KJ, Giblin AE, Shaver GR, Linkins Ae (1992) Microbial processes and plant nutrient availability in arctic soils. In: Chapin FS III, Jefferies RL, Reynolds JF, Shaver GR, Svoboda J (eds) Arctic ecosystems in a changing climate: an ecophysiological perspective. Academic Press, San Diego, pp 281–300

Oberbauer SF, Dawson TE (1992) Water relations of arctic vascular plants. In: Chapin FS III, Jefferies RL, Reynolds JF, Shaver GR, Svoboda J (eds) Arctic ecosystems in a changing climate: an ecophysiological perspective. Academic Press, San Diego, pp 259–280

Ostendorf B, Reynolds JF (1993) Relationships between a terrain-based hydrologic model and patch-scale vegetation patterns in an arctic tundra landscape. Landscape Ecol 8: 229–237

Ostendorf B, Reynolds JF (1996) A model of arctic tundra vegetation derived from topographic gradients (submitted)

Quinn P, Beven K, Chevallier P, Planchon O (1991) The prediction of hillslope flow paths for distributed hydrological modelling using digital terrain models. Hydrol Proc 5: 59–79

Reich JW, Rastetter EB, Melillo JM, Kicklighter DW, Steudler PA, Peterson BJ, Grace AL, Moore B III, Vörösmarty CJ (1991) Potential net primary productivity in South America: application of a global model. Ecol Appl 14: 399–429

Reynolds JF, Leadley PW (1992) Modeling the response of arctic plants to changing climate. In: Chapin FS III, Jefferies RL, Reynolds JF, Shaver GR, Svoboda J (eds) Arctic ecosystems in a changing climate: an ecophysiological perspective. Academic Press, San Diego pp 413–440

Romme WH (1982) Fire and landscape diversity in subalpine forests of Yellowstone National Park. Ecol Monogr 52: 199–221

Rossi RE, Mulla DJ, Journel AG, Franz EH (1992) Geostatistical tools for modeling and interpreting ecological spatial dependence. Ecol Monogr 62(2): 277–314

Santelmann MV, Gorham E (1988) The influence of airborne road dust on the chemistry of *Sphagnum* mosses. J Ecol 76:1219–1231

Sellers PJ (1987) Canopy reflectance, photosynthesis, transpiration: the role of biophysics in the linearity of their interdependence. Remote Sens Environ 21: 143–183

Shaver GR, Chapin FS III (1980) Response to fertilization by various plant growth forms in an Alaskan tundra: nutrient accumulation and growth. Ecology 61: 662–675

Shaver GR, Chapin FS III (1991) Production: biomass relationships and element cycling in contrasting arctic vegetation types. Ecol Monogr 61: 1–31

Shaver GR, Chapin FS III, Gartner BL (1986) Factors limiting seasonal growth and peak biomass accumulation in *Eriophorum vaginatum* in Alaskan tussock tundra. J Ecol 74: 257–278

Shugart HH (1984) A theory of forest dynamics. Springer, Berlin Heidelberg New York

Stow D, Burns B, Hope A (1989) Mapping arctic tundra vegetation using digital SPOT/HRV-XS data: a preliminary assessment. Int J Remote Sens 10: 1451–1457

Tehnunen JD, Lange OL, Hahn S, Siegwolf R, Oberbauer SF (1992) The ecosystem role of poikilohydric tundra plants In: Chapin FS III, Jefferies RL, Reynolds JF, Shaver GR, Svoboda J (eds) Arctic ecosystems in a changing climate: an ecophysiological perspective. Academic Press, San Diego, pp 213–238

Turner MG (ed) (1987) Landscape heterogeneity and disturbance. Springer, Berlin Heidelberg New York

Turner MG (1989) Landscape ecology: the effect of pattern on process. Annu Rev Ecol Syst 20: 171–197

Turner MG, Dale VH (1991) Modeling landscape disturbance. In: Turner MG, Gardner RH (eds) Quantitative methods in landscape ecology. Springer, Berlin Heidelberg New York, pp 323–35

Walker DA, Everett KR (1987) Road dust and its environmental impact on Alaskan taiga and tundra. Arct Alp Res 19: 479–489

Walker DA, Binnan E, Evans BM, Lederer ND, Nordstrand E, Webber PJ (1989) Terrain, vegetation, landscape evolution of the R4D research site, Brooks Range Foothills, Alaska. Holarct Ecol 12: 238–261

Wu J, Levin SA (1994) A spatial patch dynamic modeling approach to pattern and process in an annual grassland. Ecol Monogr 64: 447–464